

Complex Researches of Tropospheric and Stratospheric Ozone Performed at the Institute of Atmospheric Optics as a Basis of a Complete Radiation Experiment

V. V. Zuev

Institute of Atmospheric Optics
Siberian Branch of the Russian Academy of Sciences
Tomsk, Russia

Systematic observations of the earth's ozone layer over the last ten years indicate a steady decrease of ozone content in the stratospheric maximum and, on the contrary, a increase of ozone concentrations in the troposphere. This trend is illustrated clearly by the results of 20 years' observations of high-altitude ozone concentration distribution in the troposphere and stratosphere at Hohenpeissenberg observatory (Figure 1).

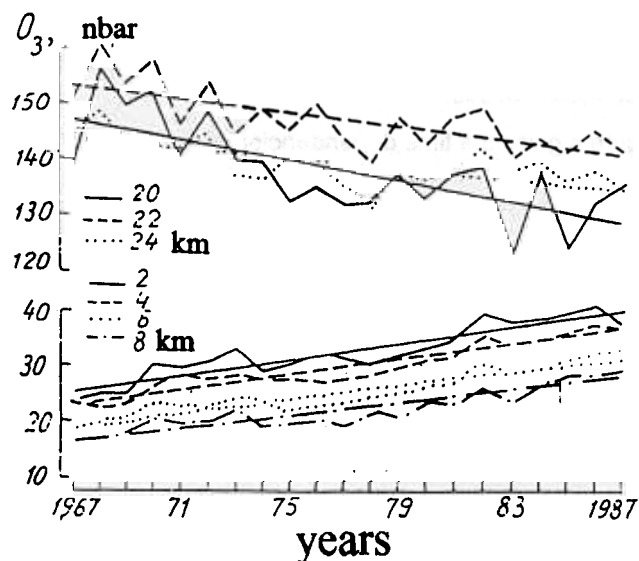


Figure 1. Twenty years' observations of stratospheric and tropospheric ozone concentrations.

In addition to photochemical and dynamical processes in the stratosphere, the decrease of stratospheric ozone content is also stimulated by high-power aerosol pollutions of the stratosphere after volcanic eruptions. The ozone layer of the stratosphere was subjected to especially strong depression after the Mt. Pinatubo eruption in the Philippine Islands in 1991 (Figure 2).

To describe the ozone cycle in the troposphere and stratosphere as a whole requires simultaneous information on a large number of gas trace species and aerosol and

Total ozone (D.U.) at January, 28, 1992

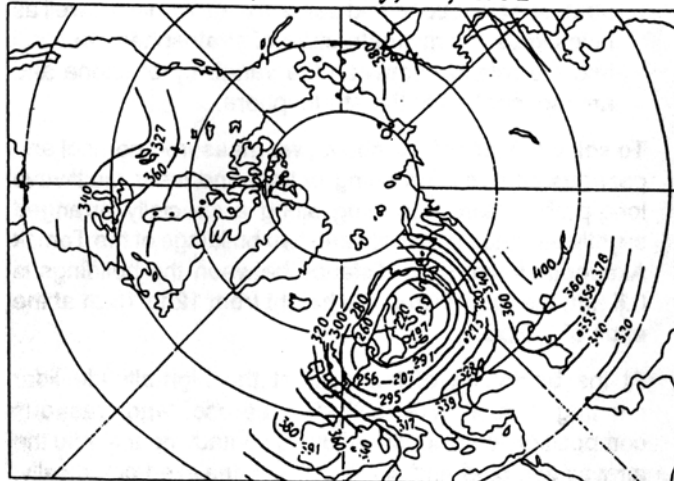


Figure 2. Stratospheric ozone layer after Mt. Pinatubo eruption.

atmospheric meteorological parameters. Some of these gases and aerosols are O_3 , N_2O , NO_x (NO , NO_2), CH_4 , nonmethane hydrocarbons ($CH_2 \dots N$), CO , CO_2 , aldehydes (H_2CO , ...), ketons, PAN (peroxyacetylenitrates), H_2O , H_2O_2 , freons ($CFCl_2(11)$, $CF_2Cl_2(12)$, ...), HCl , HF , ClO , $ClONO_2$, aerosols, meteoparameters.

In 1991 at the Institute of Atmospheric Optics, a long-term complex program on the investigation of stratospheric and tropospheric ozone, "SATOR" (Stratospheric and Tropospheric Ozone Research), was formulated.

The program's primary objective is to perform a long-term complex experiment in the atmosphere by means of a large set of different devices located in one place and to analyze a long series of synchronous atmospheric observations obtained. The structure of the SATOR program is given in Figure 3.

The primary near-term objectives of the SATOR program are the following:

- Investigate the temporal variability of ozone concentration in the lower troposphere as a function of
 - variability of the aerosol and gas composition of the atmospheric boundary layer
 - the dynamics of the atmospheric boundary layer
- Study the dynamics of the vertical distribution of stratospheric ozone and aerosol over Tomsk as well as investigate the microstructure of stratospheric aerosol and the relation between the variability of ozone and aerosol content in the stratosphere.

To solve the first of the above, we measured aerosol and gaseous composition using optical and laser multiwave long-path meters operating along a specially arranged slightly elevated path between two buildings of the Tomsk Academic town. (The distance between the buildings is 0.5 km; the meters are at a height from 12 to 18 m at the ends of the path).

At the beginning of the path at the high-altitude lidar sensing station (HALSS), the aerosol and gaseous composition was measured using contact means, and the air was sampled and subsequently analyzed chemically. Here, at two points at different altitudes, the averaged and pulsed values of temperature, wind velocity and wind direction, air humidity were measured. An acoustic sounder

(sodar) and an aerosol lidar were used to determine the altitude of the mixing layer and to study the dynamics of the atmospheric boundary layer.

To solve the second problem, we used the stationary lidars "Aeroson" and "Kolis," which have receiving telescopes with diameters of 1 and 2.2 m. Lidar sensing of the stratosphere was accompanied by launching the sounding balloons with meteo- and ozonosondes. Because of background noise, the photon-counting recording (detecting) regime of sounding laser radiation reflected by stratospheric aerosols and ozone was only at night. Originally in the process of developing the SATOR program, it was proposed to bring it closer to the total radiation experiment.

The potential of the SATOR program can be illustrated by some results presented in this paper.

Gaseous components are listed in Table 1. These components are detected by means of the laser gas analyzer "Tral." "Tral" is based on tunable CO_2 - and CO -lasers equipped with the IR parametric frequency converters made from $ZnGeP_2$ and $AgGaSe_2$ along the 1-km path length. The gas analyzer operates on the basis of the method of laser radiation differential absorption at long paths. It is sensitive enough to detect the main gases present at background concentrations. It is of principal importance that the analyzer be able to detect the main greenhouse gases.

Figure 4 gives the time dependencies of the O_3 and CO_2 concentrations measured with the use of the gas analyzer "Tral." Positive correlation is evident in the behavior of these greenhouse gases, behavior which is due to the final oxidation reaction of CO and hydroxyl OH (the main ozone destroyer in the troposphere) in the methane oxidation cycle.

Figures 5 and 6 illustrate lidar capabilities for sounding the vertical distribution of water vapor with detailed structure in the atmospheric boundary layer and up to maximum altitudes of about 17 km.

Since 1985, regular lidar observations of stratospheric aerosol have been carried out at the Institute of Atmospheric Optics, and since 1989, the stratospheric ozone has been monitored. A set of the averaged backscattering coefficients measured at a wavelength of 532 nm is presented in

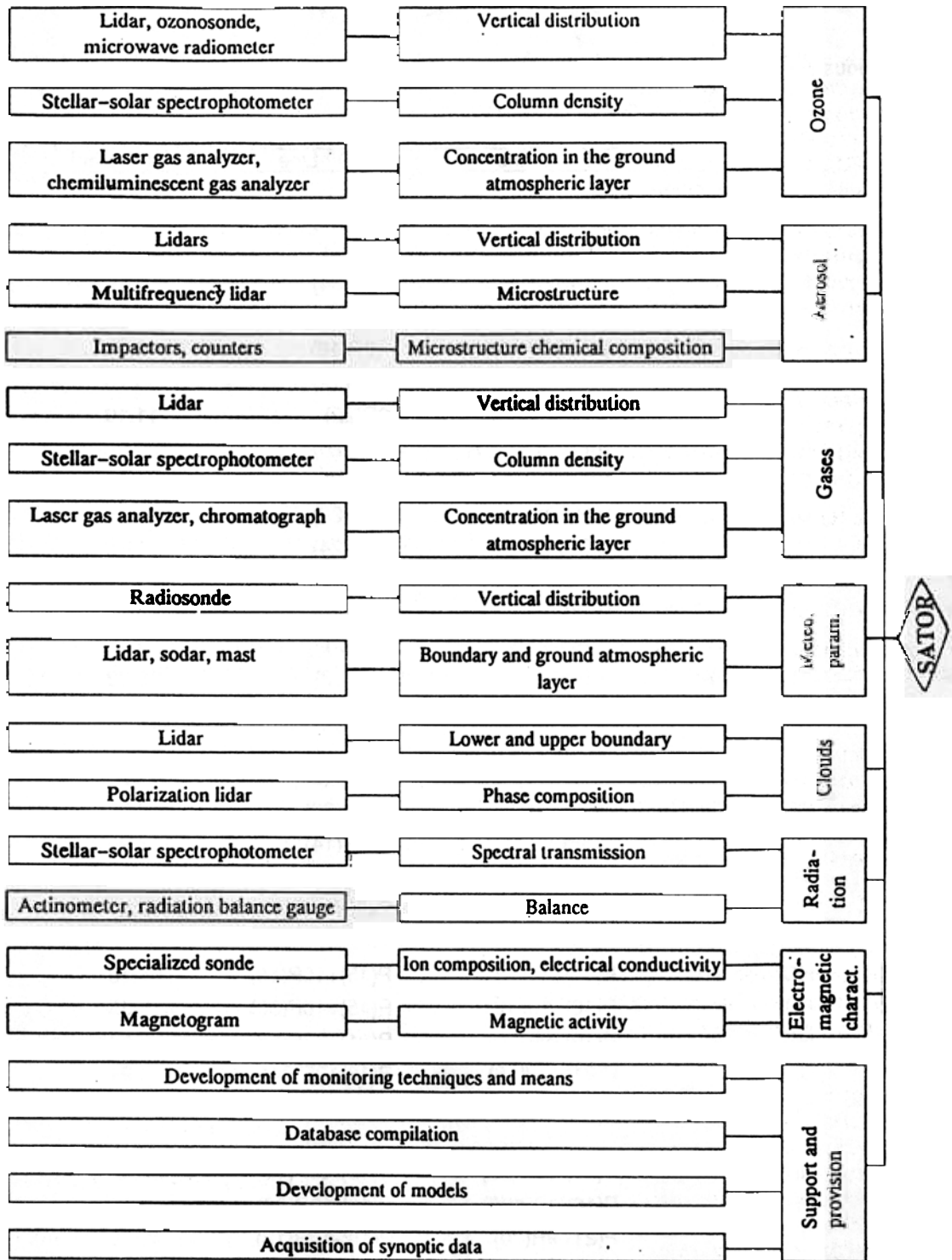


Figure 3. SATOR program structure.

Table 1. Gaseous components detected by "Tral."

Section	Gas	Lasing Lines and their Combinations		CDA cm ⁻¹ -atm ⁻¹	MDC ppb
		On-Line	Off-Line		
1	SF ₆	10P(16)	10P(10)	620.0	8(-2)
2	NH ₃	9R(30)	9R(28)	75.03	1
3	N ₂ H ₄	10P(32)	10P(34)	3.30	15
4	C ₆ H ₆	9P(30)	9P(26)	1.60	31
5	H ₂ O	10R(20)	10R(18)	0.001	165ppm
6	C ₂ H ₄	10P(14)	10P(12)	30.70	2
7	O ₃	9P(14)	9P(22)	11.10	5
8	C ₂ N ₅ SH	10R(26)	10P(20)	0.38	600
9	C ₂ H ₃ Cl	10P(22)	9R(18)	8.75	20
10	C ₂ HCl ₃	10P(20)	10R(20)	12.56	24
11	C ₂ Cl ₄	10P(34)	10R(24)	4.80	60
12	C ₂ H ₅ Cl	10R(16)	10P(20)	3.24	75
13	C ₂ H ₄ Cl ₂	10P(20)	10R(16)	0.51	550
14	C ₄ H ₅ Cl	10R(18)	9P(22)	9.05	45
15	CF ₂ Cl ₂	10P(32)	10P(12)	35.62	6
16	CFCl ₃	9R(22)	9P(18)	29.10	7
17	NO	2x10P(24)	2x10P(26)	1.98	41
18	CO	2x9P(24)	2x9P(26)	26.59	4
2 19	OCS	2x9P(30)	2x9P(14) ¹	113.9	1
20	CO ₂	10R(30)+9R(14)	2x9P(40)	0.023	4ppm
21	N ₂ O	9R(40)+9R(18) ²	2x9P(40)	18.07	6
22	HCl	P(17)+10P(32)	P(15)+10P(16)	34.10	3
3 23	HBr	P(16)+10P(24)	P(15)+10P(30)	5.35	200
24	NO ₂	P(19)+9P(20)	P(21)+10P(26)	3.66	300
25	CH ₄	P(21)+9P(16)	P(19)+9P(24)	5.94	21
26	H ₂ CO	P(17)+10R(14)	P(18)+9P(18)	20.95	6
27	HNO ₃	P(16)-10R(20)	P(15)-10P(12)	9.42	110
4 28	PH ₃	P(16)-10P(28)	P(16)-10P(26)	2.13	1ppm
29	C ₂ H ₂	P(21)-9R(30)	P(18)-10R(18)	43.99	3
30	HCN	P(99)-9R(16)	P(14)-10R(22)	10.43	110

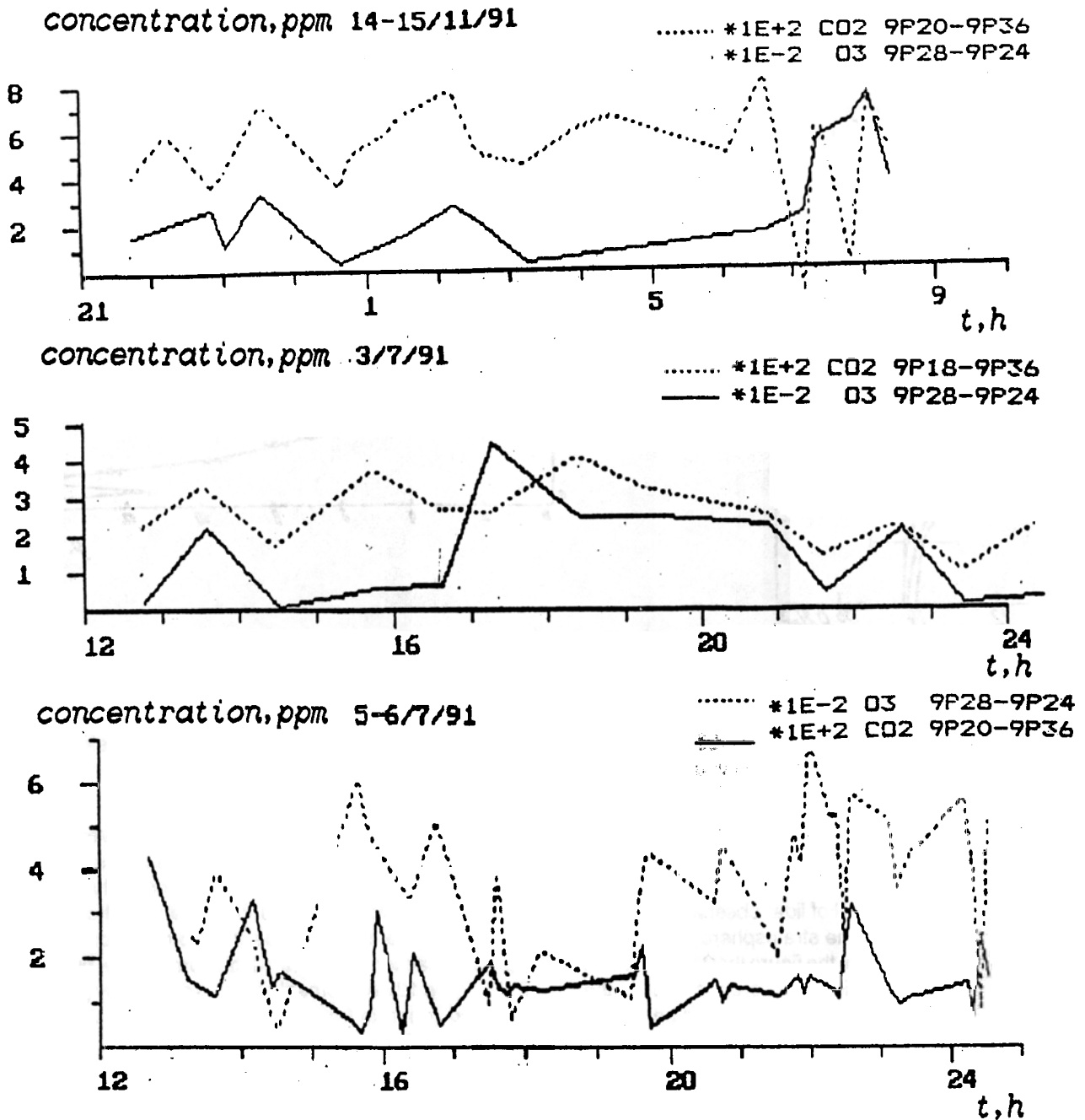


Figure 4. Time dependencies of O₃ and CO₂ concentrations measured by laser gas analyzer.

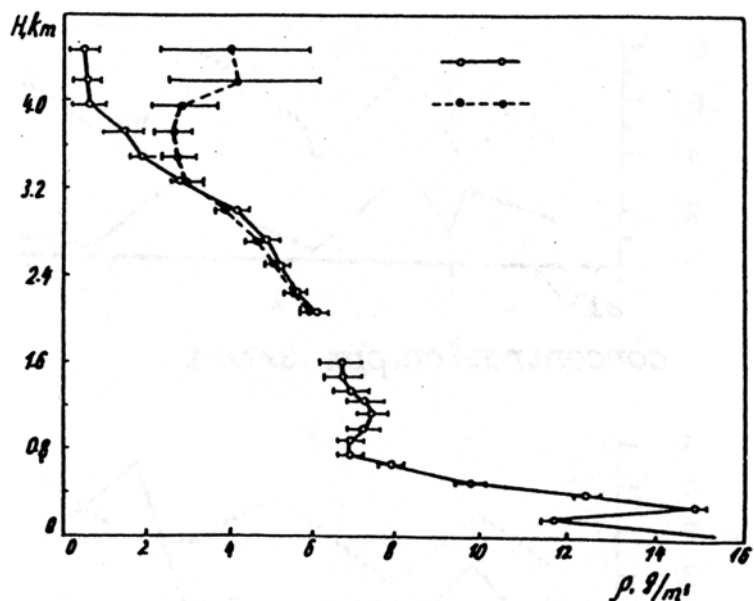
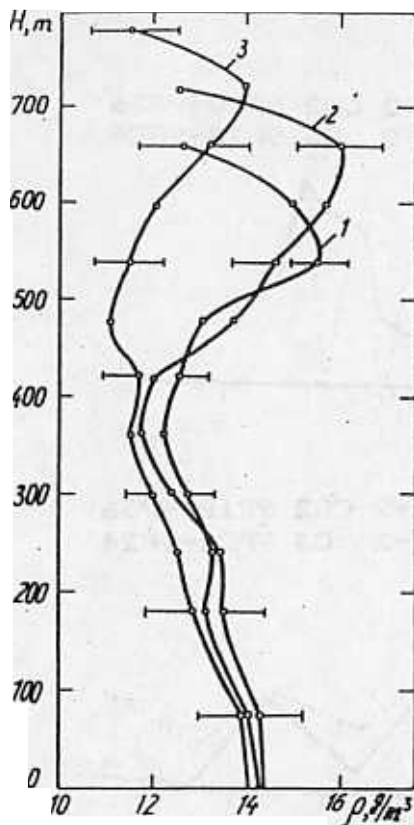


Figure 5. Vertical distribution of water vapor structure in the atmospheric boundary layer.

Figure 7. The results of simultaneous observations of stratospheric aerosol and ozone shortly after the Mt. Pinatubo eruption are shown in Figure 8. As shown in the figure, for 3 days, from July 6 until July 9, 1991, the ozone content in the stratospheric maximum decreased more than twofold.

Figure 9 shows a selective set of lidar observations of the volcanic cloud dynamics in the stratosphere over Tomsk during a year. It is evident from the figure that the maximum values of the scattering relationship were recorded at the end of January and in February 1992. Over this period the aerosol transmittance of the stratosphere decreased

(Figure 10). Mt. Pinatubo's maximum depression of the ozone layer in the stratosphere is observed during the same period (Figure 11).

In April 1992, the ozone situation stabilized even though aerosol pollution of the stratosphere remained significant. The analysis of the volcanic aerosol microstructure, based on the multiwave laser sounding data, indicated the tendency for the aerosol to be transformed from a finely dispersed fraction to a coarse dispersed one by spring 1992 (Figure 12). As aerosol particles grow, they gradually settle and separate from the stratosphere, reducing their interaction with ozone.

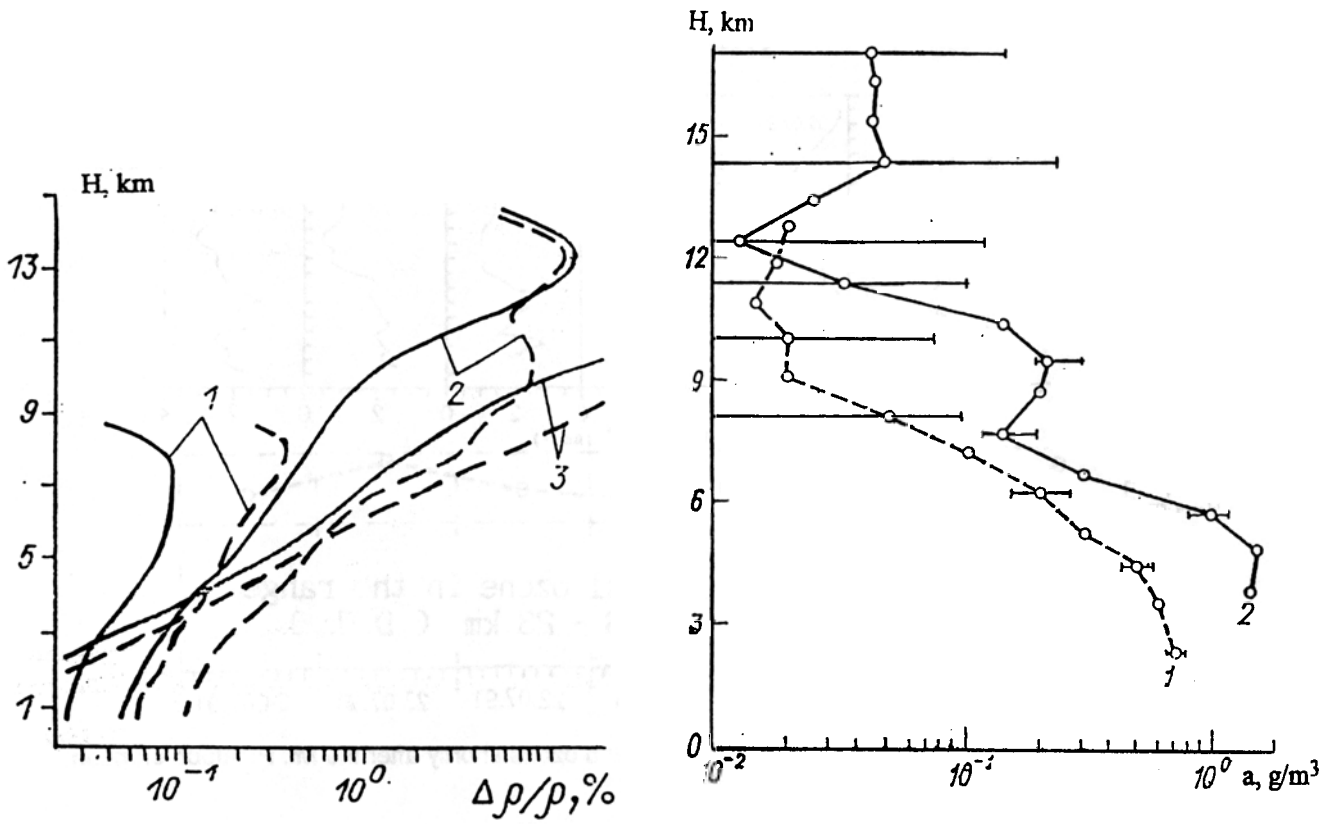


Figure 6. Vertical distribution of water vapor structure at maximum altitudes of about 17 km.

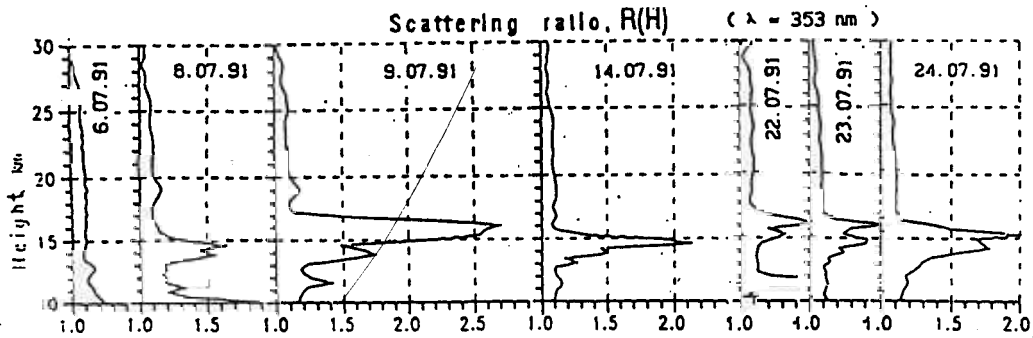


Figure 7. Averaged back-scattering coefficients measured at 532 nm.

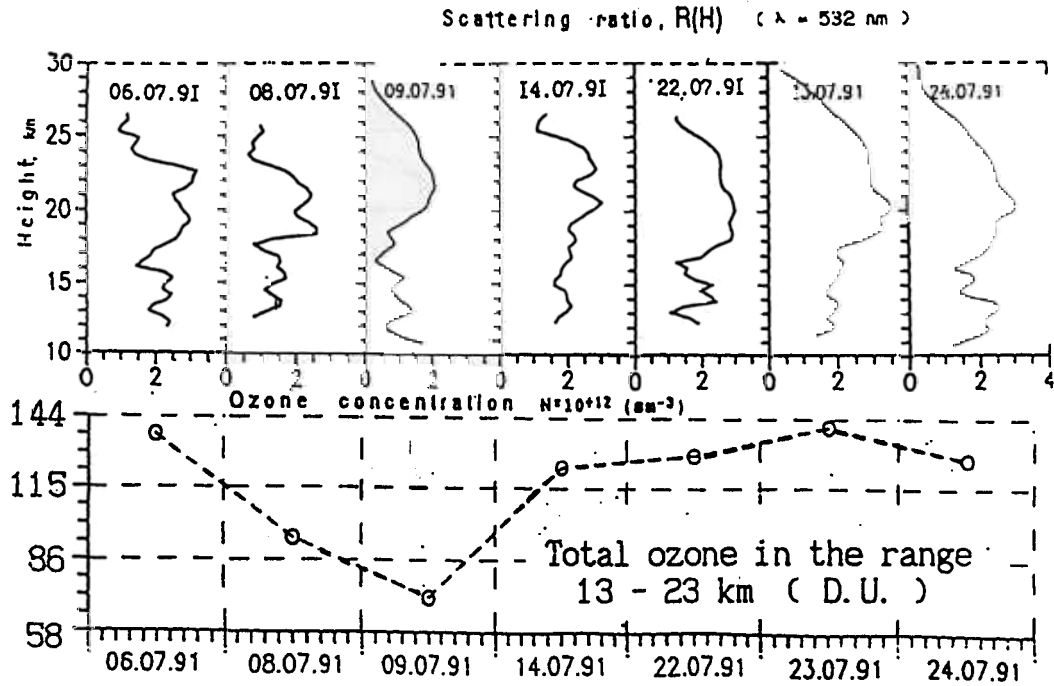


Figure 8. Simultaneous observations of stratospheric aerosol and ozone shortly after the Mt. Pinatubo eruption.

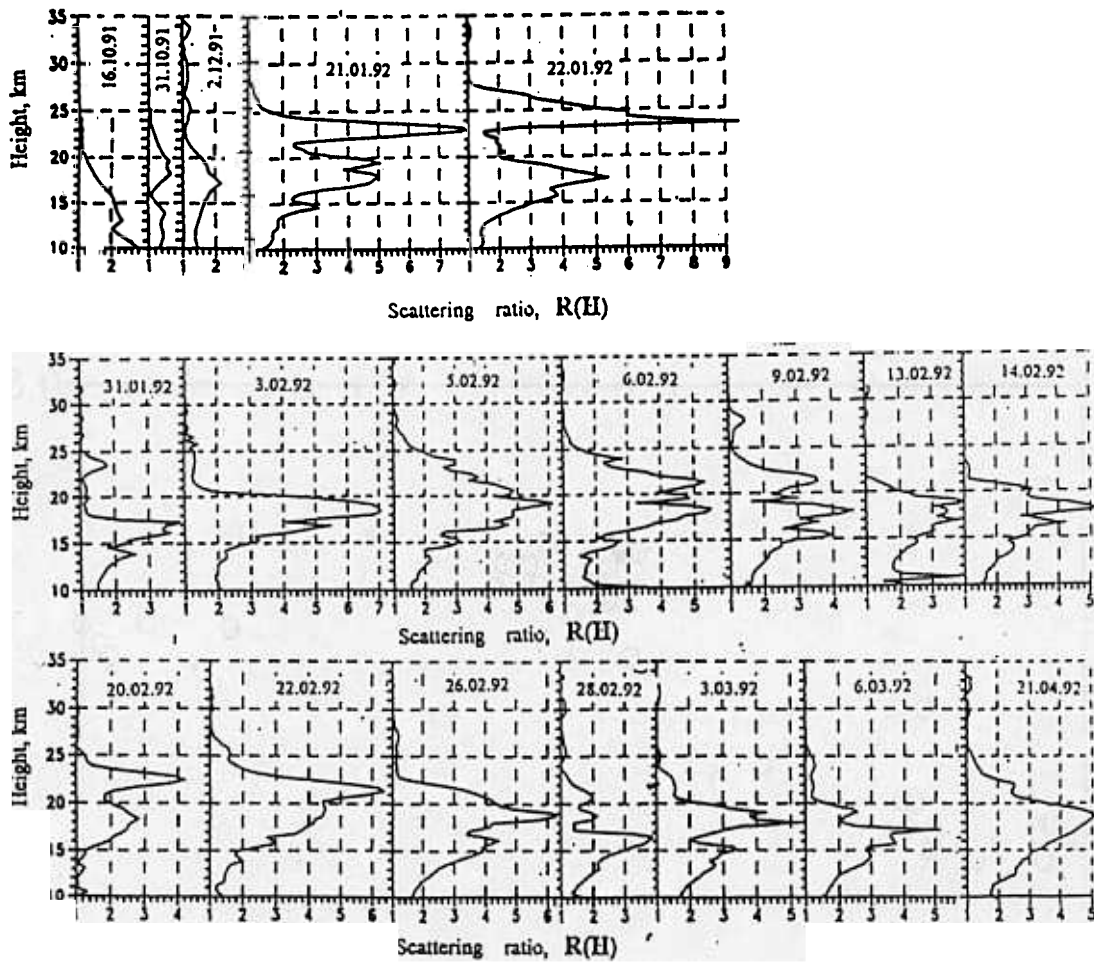


Figure 9. A selective set of lidar observations of volcanic cloud dynamics in the stratosphere over Tomsk.

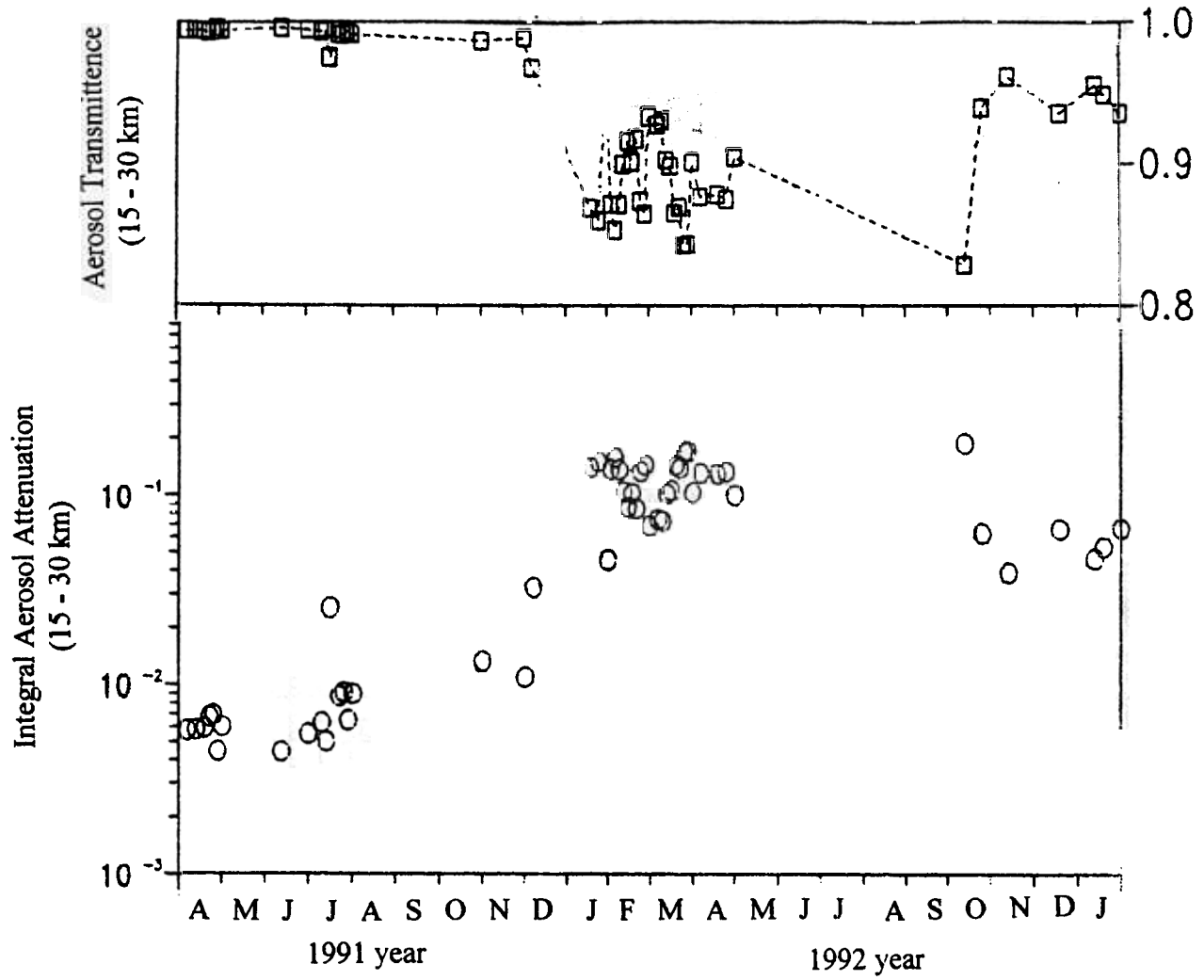


Figure 10. Decreased aerosol transmittance, January and February 1992.

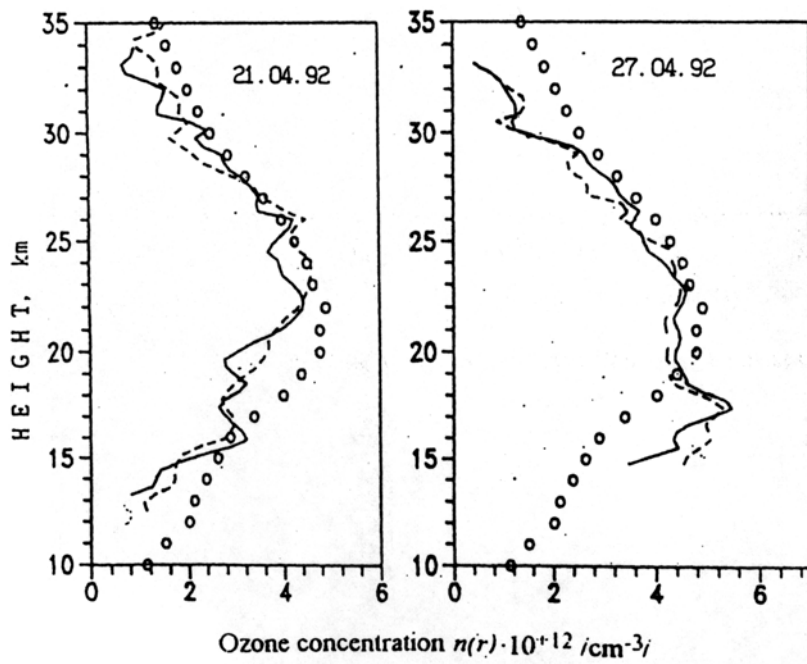
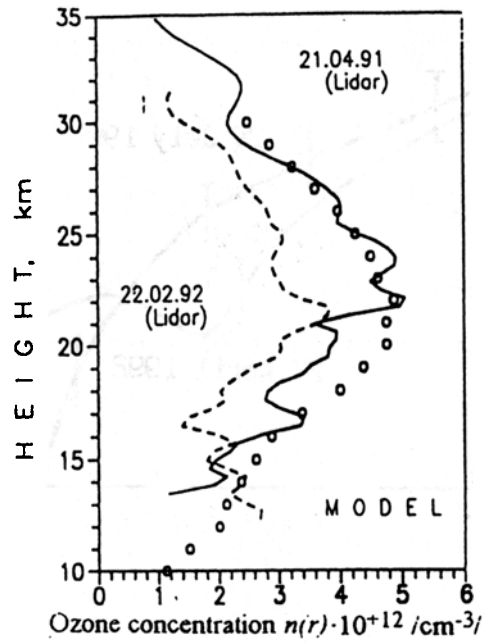


Figure 11. Effect of Mt. Pinatubo eruption on stratospheric ozone over Tomsk.

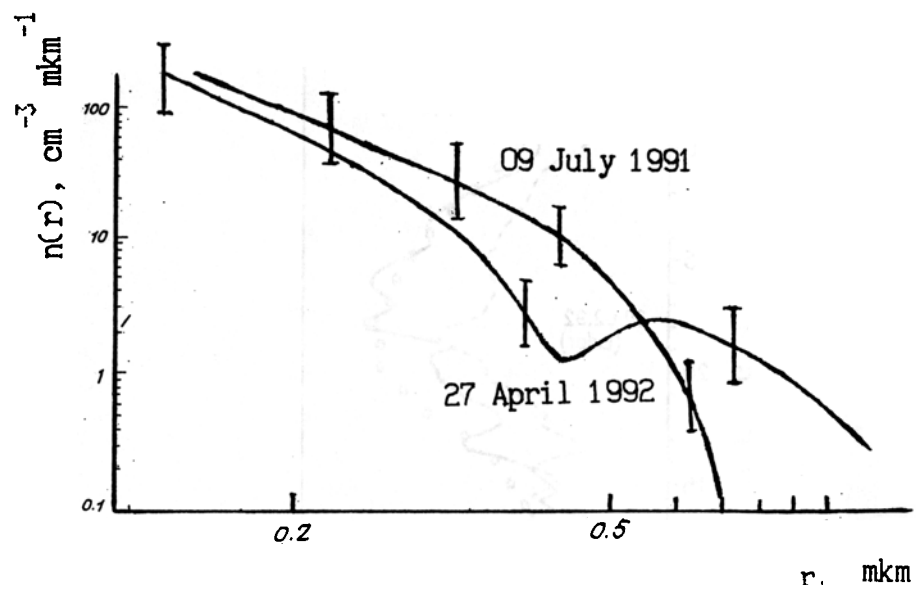


Figure 12. Aerosol transformation.